Glutamate Counteracts Dopamine/PKA Signaling via Dephosphorylation of DARPP-32 Ser-97 and Alteration of Its Cytonuclear Distribution

Akinori Nishi, Miriam Matamales, Veronica Musante, Emmanuel Valjent, Mahomi Kuroiwa, Yosuke Kitahara, Heike Rebholz, Paul Greengard, Jean-antoine Girault, Angus C. Nairn

Glutamate Counteracts Dopamine/PKA Signaling via Dephosphorylation of DARPP-32 Ser-97 and Alteration of Its Cytonuclear Distribution*

Akinori Nishi[‡1], Miriam Matamales[§2], Veronica Musante[¶], Emmanuel Valjent[‖], Mahomi Kuroiwa[‡], Yosuke Kitahara[‡], Heike Rebholz[**3], Paul Greengard[**], Jean-Antoine Girault[§], and Angus C. Nairn[¶]

From the ‡Department of Pharmacology, Kurume University School of Medicine, Kurume, Fukuoka 830-0011, Japan, §Institut du Fer à Moulin, INSERM, UPMC UMR-S839, 75005 Paris, France, ¶Department of Psychiatry, Yale University School of Medicine, New Haven, Connecticut 06508, ‖Institut de Génomique Fonctionnelle, Inserm U1191, UMR 5203 CNRS, Montpellier University, 34094 Montpellier, France, and **Laboratory of Molecular and Cellular Neuroscience, The Rockefeller University, New York, New York 10065

Edited by Roger J. Colbran

The interaction of glutamate and dopamine in the striatum is heavily dependent on signaling pathways that converge on the regulatory protein DARPP-32. The efficacy of dopamine/D1 receptor/PKA signaling is regulated by DARPP-32 phosphorylated at Thr-34 (the PKA site), a process that inhibits protein phosphatase 1 (PP1) and potentiates PKA action. Activation of dopamine/D1 receptor/PKA signaling also leads to dephosphorylation of DARPP-32 at Ser-97 (the CK2 site), leading to localization of phospho-Thr-34 DARPP-32 in the nucleus where it also inhibits PP1. In this study the role of glutamate in the regulation of DARPP-32 phosphorylation at four major sites was further investigated. Experiments using striatal slices revealed that glutamate decreased the phosphorylation states of DARPP-32 at Ser-97 as well as Thr-34, Thr-75, and Ser-130 by activating NMDA or AMPA receptors in both direct and indirect pathway striatal neurons. The effect of glutamate in decreasing Ser-97 phosphorylation was mediated by activation of PP2A. In vitro phosphatase assays indicated that the PP2A/PR72 heterotrimer complex was likely responsible for glutamate/Ca^{2+}-regulated dephosphorylation of DARPP-32 at Ser-97. As a consequence of Ser-97 dephosphorylation, glutamate induced the nuclear localization in cultured striatal neurons of dephospho-Thr-34/dephospho-Ser-97 DARPP-32. It also reduced PKA-dependent DARPP-32 signaling in slices and in vivo. Taken together, the results suggest that by inducing dephosphorylation of DARPP-32 at Ser-97 and altering its cytonuclear distribution, glutamate may counteract dopamine/D1 receptor/PKA signaling at multiple cellular levels.

Dopamine and cAMP-regulated phosphoprotein of M_r 32,000 (DARPP-32) plays an essential role in dopamine/D1 receptor/PKA signaling in striatal medium spiny neurons (1–4). DARPP-32 is phosphorylated at Thr-34 by PKA, converting it into a potent inhibitor of protein phosphatase 1 (PP1).[4] Thus, when PKA is activated in striatal neurons, the combined inhibition of PP1 increases the phosphorylation of substrates for both PKA and PP1. These substrates include various neurotransmitter receptors (e.g. AMPA GluR1 subunit, NMDA NR1 subunit, and $GABA_A$ $\beta1/\beta2$ subunits), ion channels (e.g. L/N/P-type Ca^{2+} channels, and Na^+ channel), Na^+,K^+-ATPase, and transcription factors (e.g. CREB (cAMP-response element-binding protein)), leading to regulation of excitability and gene expression (e.g. c-Fos, ΔfosB, Zif-268).

In addition to PKA, DARPP-32 is phosphorylated at other sites by several other protein kinases. A large number of studies suggest that the states of phosphorylation of the various sites in DARPP-32 are regulated by the balance of the activities of the relevant kinases and phosphatases (1–4). Thr-75 in DARPP-32 is phosphorylated by cyclin-dependent kinase 5 (Cdk5), Ser-97 by CK2, and Ser-130 by CK1. Phosphorylation of DARPP-32 at Thr-75 by Cdk5 causes inhibition of PKA (5). However, when dopamine D1 receptor/PKA signaling is activated, phospho-Thr-75 DARPP-32 is dephosphorylated via activation of PP2A/B56δ, resulting in de-inhibition of PKA and further amplification of dopamine D1 signaling (6, 7). Phosphorylation of DARPP-32 at Ser-97 by CK2 increases the efficacy of DARPP-32 Thr-34 phosphorylation by PKA (8, 9), whereas phosphorylation of DARPP-32 at Ser-130 by CK1 decreases the rate of dephosphorylation of Thr-34 by calcineurin (9). In addition, phospho-Ser-97 DARPP-32 regulates nuclear export of DARPP-

32. Notably, PKA activation also induces dephosphorylation of DARPP-32 at Ser-97 by PP2A/B56δ, resulting in nuclear accumulation of phospho-Thr-34/dephospho-Ser-97 DARPP-32, leading to PP1 inhibition in the nucleus, histone H3 phosphorylation, and transcriptional activation (10). Phosphorylation of Ser-97 also increases interaction of DARPP-32 with adducin and can thus facilitate its regulation by DARPP-32 (11). PP2C is also implicated in the dephosphorylation of DARPP-32 at Thr-75 (6) and Ser-130 (9).

The phosphorylation and dephosphorylation of the various sites of DARPP-32 play a critical role in the integration of dopamine and glutamate signaling (1–4). Earlier studies in striatal slices found that calcineurin (PP2B) mediates certain Ca^{2+}-dependent actions of glutamate to counteract dopamine D1 receptor/PKA/DARPP-32 signaling by dephosphorylating DARPP-32 at Thr-34 (12, 13). However, subsequent studies found that the actions of glutamate on DARPP-32 phosphorylation are complex. *In vivo*, glutamate and dopamine can act in a synergistic, coincident manner to activate the ERK MAP kinase pathway (14). In striatal slices, glutamate can induce a rapid increase in Thr-34 phosphorylation via activation of NMDA/AMPA receptor and mGluR5/neuronal NOS/NO/cGMP/PKG signaling that is then followed by a decrease in Thr-34 phosphorylation via activation of NMDA/AMPA receptor/intracellular Ca^{2+}/calcineurin signaling (13, 15). Following these changes, activation of mGluR5/ERK/adenosine A_{2A} receptor/PKA (16) and mGluR5/phospholipase C/CK1/phospho-Ser-130 DARPP-32 signaling (15, 17) then induces a gradual increase in Thr-34 phosphorylation. DARPP-32 Thr-75 phosphorylation is also regulated by multiple dopamine and glutamate-dependent mechanisms (6, 7, 15, 17–19). Both PP2A/B56δ (7) and PP2A/PR72 (18) dephosphorylate phospho-Thr-75 DARPP-32 after activation of PKA or Ca^{2+} signaling, respectively (6, 19). Thus, glutamate modulates cytoplasmic dopamine D1 receptor/DARPP-32 signaling in both negative and positive directions via activation of NMDA/AMPA receptor and mGluR signaling. However, it is not known how glutamate affects the phosphorylation state of DARPP-32 at Ser-97 nor how it modulates the localization and function of DARPP-32 in the nucleus. In this study we first characterized the glutamate-induced phosphorylation profile of DARPP-32 including Ser-97 in striatal slices and then investigated the role of glutamate in the regulation of DARPP-32 nuclear translocation. The results suggest that glutamate-dependent dephosphorylation of Ser-97 can lead to nuclear sequestration of an inactive form of DARPP-32 and highlights the existence of multiple modes of DARPP-32 regulation by which glutamate can oppose dopamine signaling.

Results

Role of Glutamate in the Regulation of DARPP-32 Phosphorylation in Striatal Slices—Although we have previously carried out detailed studies of the phosphorylation and dephosphorylation of DARPP-32, the conditions varied between the various experiments and focused largely on Thr-34 and Thr-75. To obtain a comprehensive profile of the regulation of DARPP-32 phosphorylation at all sites under the same conditions, we first

carried out a parallel analysis of the effects of glutamate in striatal slices (Fig. 1).

Treatment of striatal slices with glutamate (5 mM) rapidly and transiently increased DARPP-32 Thr-34 phosphorylation at 15 s of incubation (Fig. 1A), presumably due to activation of neuronal NOS/NO/cGMP/PKG signaling (15, 20). Glutamate subsequently decreased Thr-34 phosphorylation below the basal level at 2 and 5 min of incubation due to activation of calcineurin (15), and then the decreased Thr-34 phosphorylation returned to the basal level at 10 min due to activation of mGluR5 (15, 17). Treatment with glutamate decreased DARPP-32 Thr-75 phosphorylation at 2 and 5 min of incubation (Fig. 1B). The decrease is likely mediated through dephosphorylation of Thr-75 by Ca^{2+}-activated PP2A/PR72 (15, 18). Treatment with glutamate also decreased DARPP-32 Ser-97 phosphorylation to ~50% of control by 2 min of incubation, and further decreased phosphorylation to 20% of control at 10 min of incubation (Fig. 1C). Glutamate also decreased DARPP-32 Ser-130 phosphorylation after 10 min of incubation, but the decrease (50% of control) was less than for Ser-97 (Fig. 1D).

To compare the phosphorylation profiles of DARPP-32 after activation of glutamate/Ca^{2+} and PKA signaling, we also examined the effects on DARPP-32 phosphorylation of forskolin, which activates adenylyl cyclase and thus stimulates PKA (Fig. 1, E–H). Treatment of striatal slices with forskolin (1 μM) increased DARPP-32 Thr-34 phosphorylation by 8-fold at 10 min of incubation (Fig. 1E). In contrast, forskolin decreased Thr-75 and Ser-97 phosphorylation (Fig. 1, F and G) presumably due to activation of dephosphorylation by PP2A/B56δ (6, 7, 10). Forskolin did not affect the levels of phospho-Ser-130 DARPP-32 (Fig. 1H), suggesting that CK1 kinase activity is not modulated by PKA and that phospho-Ser-130 DARPP-32 is not a substrate for PP2A/B56δ, in agreement with previous reports indicating the role of PP2C in neurons (21). Thus, activation of glutamate/Ca^{2+} signaling and PKA signaling results in distinct profiles of DARPP-32 phosphorylation (see also the model shown below in Fig. 10A).

Role of NMDA and AMPA Receptors in the Regulation of DARPP-32 Phosphorylation—Treatment of striatal slices with an NMDA receptor agonist, NMDA (100 μM), decreased DARPP-32 phosphorylation at all sites: after 2 min at Thr-34, Thr-75, and Ser-97 and after 10 min at Ser-130 (Fig. 1, I–L). The NMDA-induced decreases in the phosphorylation at the four sites were blocked by NMDA receptor antagonists, MK801 (100 μM) and AP5 (100 μM) (data not shown). The rapid increases in phosphorylation at the four sites, observed at 15 s of incubation with NMDA, were relatively small and were significant only at Ser-97. Treatment with an AMPA receptor agonist, AMPA (100 μM), also decreased DARPP-32 phosphorylation at the four sites (Fig. 1, M–P). AMPA also induced the rapid increase in Thr-34 phosphorylation at 15 and 30 s of incubation, as observed with glutamate treatment (Fig. 1A). The AMPA-induced decreases in the phosphorylation at the four sites were prevented by an AMPA receptor antagonist, NBQX (20–100 μM) (data not shown).
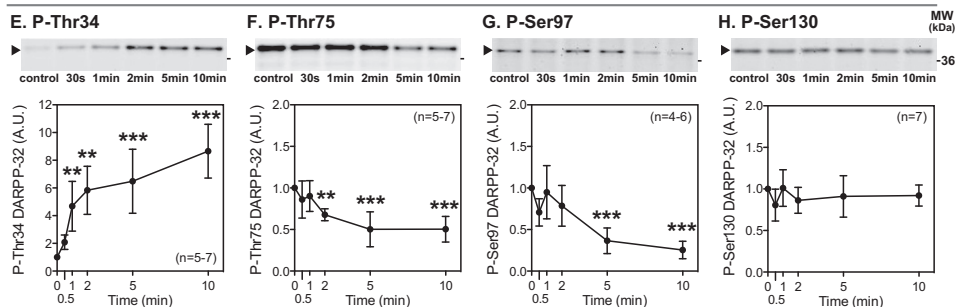
The effects of glutamate (5 mM) were examined in the presence of an NMDA receptor antagonist (MK801) plus an AMPA
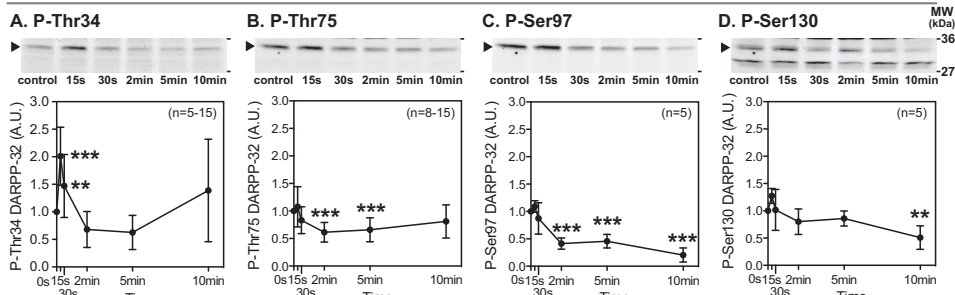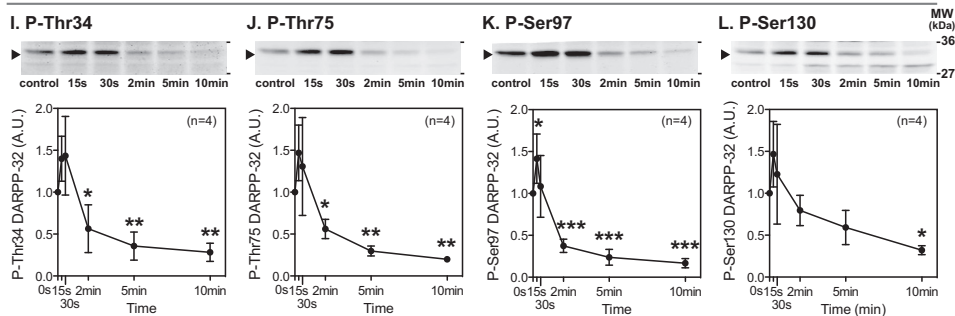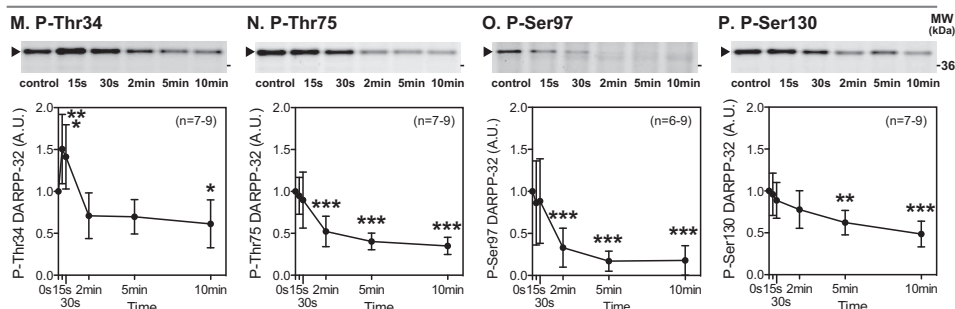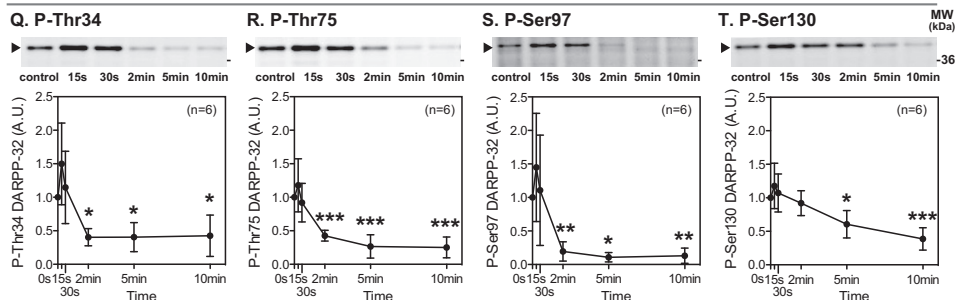
A-B. Glutamate + MK801/CNQX
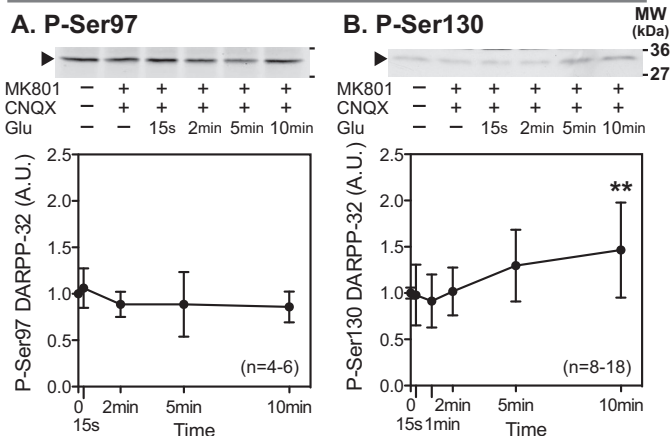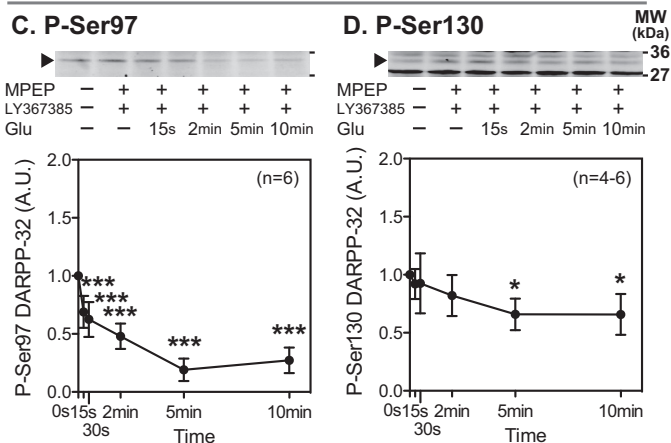
FIGURE 2. Effects of glutamate in the presence of antagonists for NMDA and AMPA receptors or group I mGluRs. Striatal slices were preincubated with an NMDA receptor antagonist, MK801 (100 μM) plus an AMPA receptor antagonist, CNQX (20 μM) (*A* and *B*), or an mGluR5 antagonist, MPEP (10 μM) plus an mGluR1 antagonist, LY367385 (100 μM) (*C* and *D*), for a total of 20 min with the addition of glutamate (5 mM) for the indicated times. Phosphorylation of DARPP-32 at Ser-97 (the CK2 site) and Ser-130 (the CK1 site) was determined by immunoblotting. Data represent the means $\pm$ S.D. The number of experiments is indicated in *parentheses*. *, $p < 0.05$; **, $p < 0.01$; ***, $p < 0.001$ compared with control slices; one-way ANOVA followed by Newman-Keuls test. *A.U.*, arbitrary units.

receptor antagonist (CNQX) (Fig. 2, *A* and *B*) or an mGluR5 antagonist (MPEP) plus an mGluR1 antagonist (LY367385) (Fig. 2, *C* and *D*). In striatal slices pretreated with MK801 plus CNQX, glutamate had no effect on Ser-97 phosphorylation but increased Ser-130 phosphorylation. In contrast, pretreatment with MPEP plus LY367385 did not affect the glutamate-induced dephosphorylation of Ser-97 or Ser-130. Together the results suggest that glutamate induces the decrease in DARPP-32 Ser-97 phosphorylation via activation of NMDA or AMPA receptors. Regarding Ser-130, glutamate likely induces

the decrease in DARPP-32 Ser-130 phosphorylation via activation of NMDA or AMPA receptors and the increase in Ser-130 phosphorylation via activation of mGluR5 or mGluR1, which is supported by our previous study showing group I mGluRs (mGluR5 and mGluR1)-induced Ser-130 phosphorylation via activation of CK1 (17).

The NMDA- or AMPA-induced decreases in DARPP-32 phosphorylation at the four sites are presumably mediated through an increase in intracellular Ca^{2+}. We examined whether depolarization with a high concentration of KCl mimicked the effects of NMDA and AMPA. Treatment with KCl (40 mM) decreased the phosphorylation of DARPP-32 at each of the four sites (Fig. 1, *Q*–*T*) similarly to NMDA or AMPA treatment, supporting the conclusion that Ca^{2+}-dependent mechanisms are involved in the decreases in phosphorylation mediated by glutamate.

Role of Protein Phosphatases in AMPA-induced Decreases in DARPP-32 Phosphorylation—The effects of a PP2A inhibitor, okadaic acid, on the AMPA-induced decrease in DARPP-32 phosphorylation were examined (Fig. 3, *A*–*D*). Okadaic acid alone (1, 3, and 10 μM) increased the levels of phosphorylated DARPP-32 at each of the four sites. Preincubation with okadaic acid did not attenuate the effects of AMPA on phospho-Thr-34 DARPP-32 but attenuated or abolished the AMPA-induced decreases in Thr-75 and Ser-130 phosphorylation. Although okadaic acid at 1 and 3 μM failed to attenuate the effects of AMPA on Ser-97 phosphorylation, at a higher concentration (10 μM) it attenuated the effects of AMPA. Okadaic acid alone at 1 and 3 μM increased Ser-97 phosphorylation, but this effect was less pronounced and not significant at 10 μM. An inhibitor of calcineurin, cyclosporin A, increased the basal levels of phospho-Thr-34 DARPP-32 and attenuated the effect of AMPA on Thr-34 phosphorylation, whereas it did not affect the basal levels of phospho-Thr-75, Ser-97, or Ser-130 or the AMPA-induced decreases in the phosphorylation of these residues (data not shown).

Analyses of dose responsiveness to AMPA revealed that phospho-Ser-97 was sensitive to lower concentrations of AMPA compared with the other sites (Fig. 3, *E*–*H*). AMPA decreased DARPP-32 phosphorylation in a dose-dependent manner, with half-maximal effects at ~2 μM for Thr-34, Thr-75, and Ser-130 and at ~0.7 μM for Ser-97. AMPA at high concentrations (10 and 100 μM) decreased the levels of phospho-Thr-34, Thr-75, and Ser-130 to 40–50% that of control, but the level of phospho-Ser-97 was reduced to <10% of control at these concentrations.

These results suggest that the dephosphorylation machinery for Ser-97 is more sensitive to AMPA compared with the other DARPP-32 sites. The effect of AMPA on Thr-34 dephosphorylation is likely mediated through activation of calcineurin, whereas those on Thr-75 and Ser-130 dephosphorylation most

FIGURE 1. Effects of glutamate, NMDA, AMPA, KCl, and forskolin on DARPP-32 phosphorylation at four major phosphorylation sites in striatal slices. Slices from the dorsal striatum were treated with glutamate (5 mM) (*A*–*D*), forskolin (1 μM) (*E*–*H*), NMDA (100 μM) (*I*–*L*), AMPA (100 μM) (*M*–*P*), or KCl (40 mM) (*Q*–*T*) for the indicated times. Changes in the phosphorylation of DARPP-32 at Thr-34 (the PKA site), Thr-75 (the Cdk5 site), Ser-97 (the CK2 site), and Ser-130 (the CK1 site) were determined by immunoblotting using phosphorylation state-specific antibodies. Typical immunoblots are shown at the *top* of each graph. Where samples were separated using 4–12% polyacrylamide Bis-Tris gels, molecular weight markers are indicated with *asterisks*. The data were normalized to values obtained from untreated slices. Data represent the means $\pm$ S.D. The number of experiments is indicated in *parentheses*. *, $p < 0.05$; **, $p < 0.01$; ***, $p < 0.001$ compared with control slices; one-way ANOVA followed by Newman-Keuls test. *A.U.*, arbitrary units.

A-D. sensitivity of AMPA-induced dephosphorylation to okadaic acid
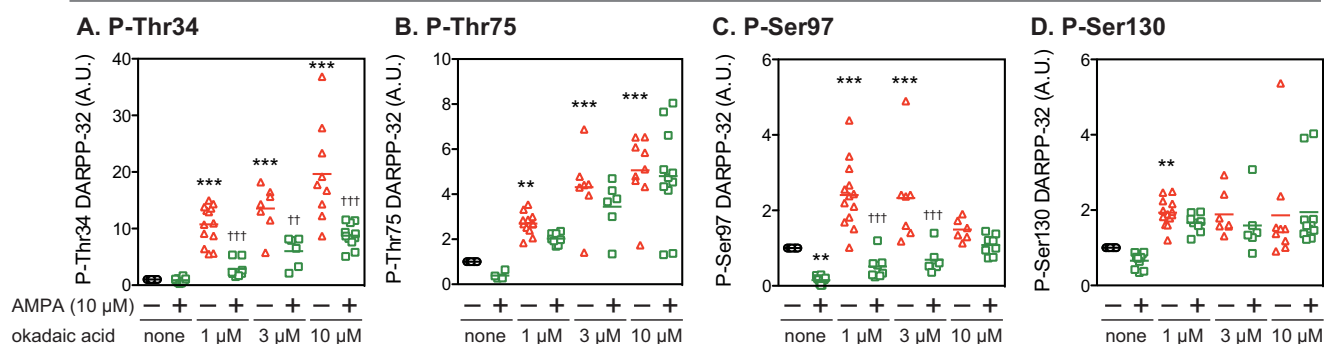
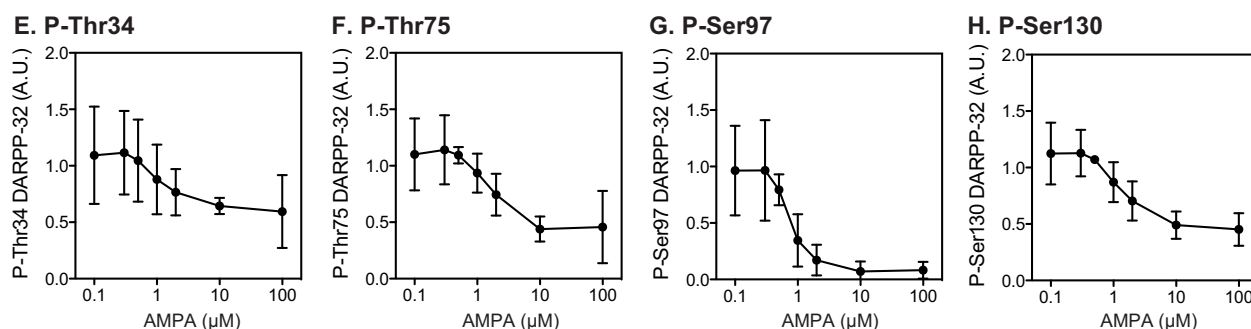**E-H. dose-dependent effect of AMPA**

FIGURE 3. **Effects of okadaic acid on AMPA-induced dephosphorylation of DARPP-32 at four phosphorylation sites.** *A–D*, striatal slices were incubated with okadaic acid at 1, 3, or 10 μM for a total of 70 min, with the addition of AMPA (10 μM) for the final 10 min. Phosphorylation of DARPP-32 at the four indicated sites was determined by immunoblotting as in Fig. 1. Data for 6–13 experiments are presented in scatter plots with the mean values indicated by a line. **, $p < 0.01$; ***, $p < 0.001$ compared with untreated slices; ††, $p < 0.01$; †††, $p < 0.001$ compared with okadaic acid alone at the same concentrations; one-way ANOVA followed by Newman-Keuls test. *E–H*, striatal slices were treated with AMPA at various concentrations (0.1–100 μM) for 10 min. Phosphorylation of DARPP-32 at the four indicated sites was determined by immunoblotting. Data represent the means ± S.D. for 3–12 experiments. *A.U.*, arbitrary units.

likely involve PP2A. Interestingly, Ser-97 dephosphorylation can clearly be mediated by PP2A based on the basal effect of okadaic acid. However, AMPA-induced Ser-97 dephosphorylation is much less sensitive to okadaic acid compared with the other two PP2A sites, Thr-75 and Ser-130. Taken together these results suggest some differences in the detailed mechanisms involved in PP2A actions on DARPP-32 depending on the target phosphorylated residues.

Regulation of DARPP-32 Phosphorylation by Glutamate in Striatonigral and Striatopallidal Neurons—We next examined whether activation of NMDA or AMPA receptors decreased DARPP-32 phosphorylation in D1 receptor-enriched striatonigral and/or D2 receptor-enriched striatopallidal neurons using striatal slices from D1-DARPP-32-FLAG/D2-DARPP-32-Myc mice (22). Immunohistochemical analyses have revealed that FLAG- and Myc-tagged DARPP-32 are segregated in two types of medium spiny neurons (12, 22), although a small population (5%) of medium spiny neurons presumably express both types of DARPP-32 (23). FLAG- and Myc-tagged DARPP-32 were independently immunoprecipitated from striatonigral and striatopallidal neurons, respectively, and the phosphorylation state of DARPP-32 at the four sites in the two types of neurons was analyzed (Fig. 4). Treatment with NMDA (100 μM) or AMPA (10 μM) decreased the phosphorylation of both FLAG- and Myc-tagged DARPP-32 at all four sites. The effects of NMDA and AMPA on the phosphorylation at Thr-75, Ser-97, and Ser-130 were similar in striatonigral and striatopallidal neurons,

whereas the effects on the phosphorylation at Thr-34 were smaller in striatonigral neurons than in striatopallidal neurons (two-way ANOVA: interaction between cell type and treatment, F value = F(degree of freedom for the between group, degree of freedom for the within group) = $F_{2,30}$ = 13.85, $p < 0.001$; effect of treatment, $F_{2,30} = 47.00$, $p < 0.001$; effect of cell type $F_{1,30} = 47.00$, $p < 0.001$; Bonferroni post-test, $p < 0.001$ FLAG- *versus* Myc-tagged DARPP-32 for both NMDA and AMPA.

CK2 Activity Is Not Regulated by Activation of NMDA or AMPA Receptors—Because Ser-97 is phosphorylated by CK2 (8), which is highly expressed in striatal neurons (24) and because dephosphorylation of Ser-97 was only poorly inhibited by okadaic acid, we examined whether activation of NMDA or AMPA receptors regulates CK2 activity in striatal slices. CK2 activity either in cytosolic or nuclear fractions was unaffected by treatment with NMDA or AMPA (Fig. 5). The results suggest that the regulation of CK2 activity is not involved in the NMDA and AMPA receptor-induced decreases in Ser-97 phosphorylation.

Phospho-Ser-97 DARPP-32 Is a Substrate for PP2A/PR72—The ability of PP2A heterotrimers to dephosphorylate phospho-Ser-97 DARPP-32 was examined *in vitro*. All three PP2A heterotrimers containing Bα, B56δ, or PR72 exhibited phosphatase activity toward Ser-97, but PP2A/PR72 showed the highest activity among the three PP2A heterotrimers (Fig. 6*A*). The phosphatase activity of PP2A/PR72 against Ser-97 was
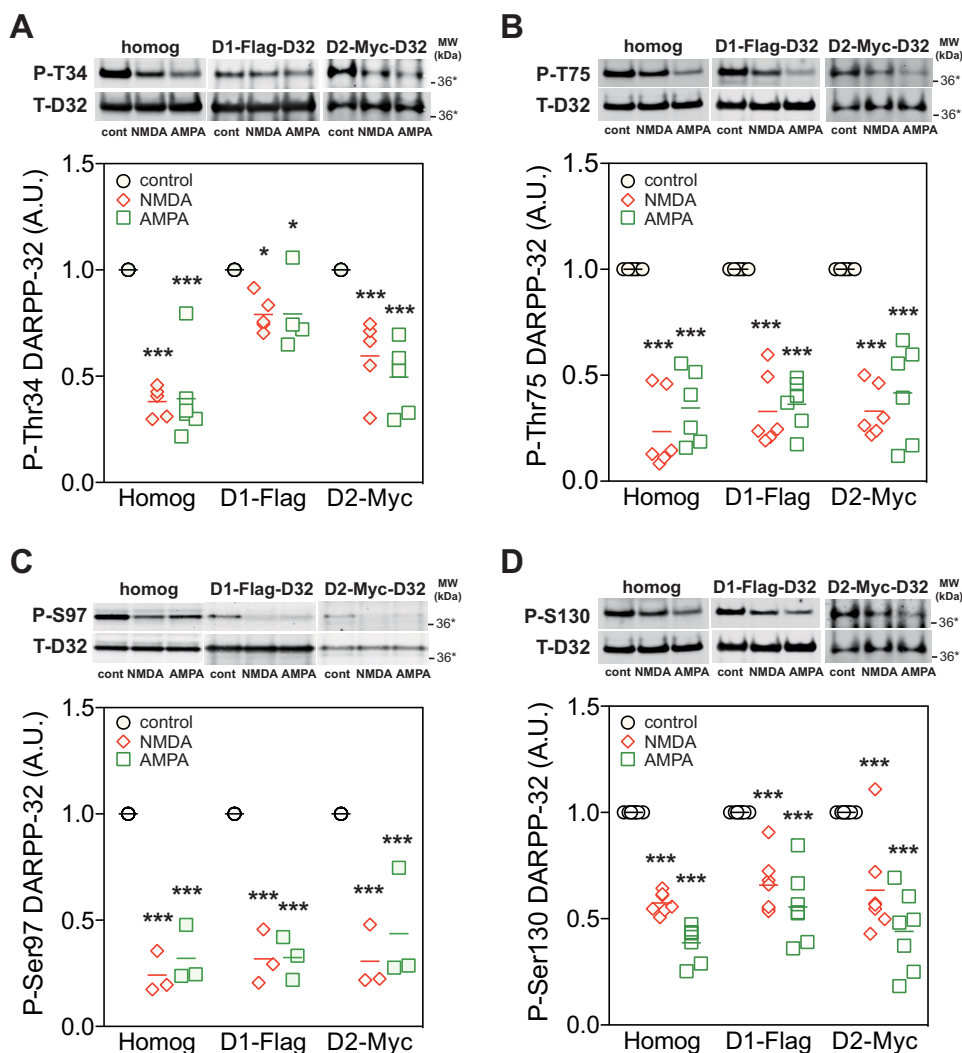
FIGURE 4. **Neuronal type-specific regulation of DARPP-32 dephosphorylation by NMDA and AMPA receptor agonists in striatal slices from D₁-DARPP-32-FLAG/D₂-DARPP-32-Myc mice.** Slices from the dorsal striatum of D_1-DARPP-32-FLAG/D_2-DARPP-32-Myc mice were incubated with NMDA (100 μM) or AMPA (10 μM) for 10 min. FLAG-tagged DARPP-32, expressed in D1 receptor-enriched striatonigral neurons, and Myc-tagged DARPP-32, expressed in D2 receptor-enriched striatopallidal neurons, were immunoprecipitated, and the phosphorylation of FLAG- and Myc-tagged DARPP-32 at the four sites was analyzed. Panels show data from total striatal homogenate (*homog*), FLAG-tagged DARPP-32 in striatonigral neurons (*D1-FLAG*), and Myc-tagged DARPP-32 in striatopallidal neurons (*D2-Myc*). Typical immunoblots for detection of phospho-Thr-34 (*P-T34*) (*A*), phospho-Thr-75 (*P-T75*) (*B*), phospho-Ser-97 (*P-S97*) (*C*), phospho-Ser-130 (*P-S130*) (*D*), and total DARPP-32 (*T-D32*) are shown at the *top of each panel*. The data (phospho-DARPP-32/total DARPP-32) were normalized to values obtained with control slices in each condition. Data for 3–6 experiments are presented in scatter plots with the mean values indicated. *, $p < 0.05$; ***, $p < 0.001$ compared with control; one-way ANOVA followed by Newman-Keuls test. *A.U.*, arbitrary units.
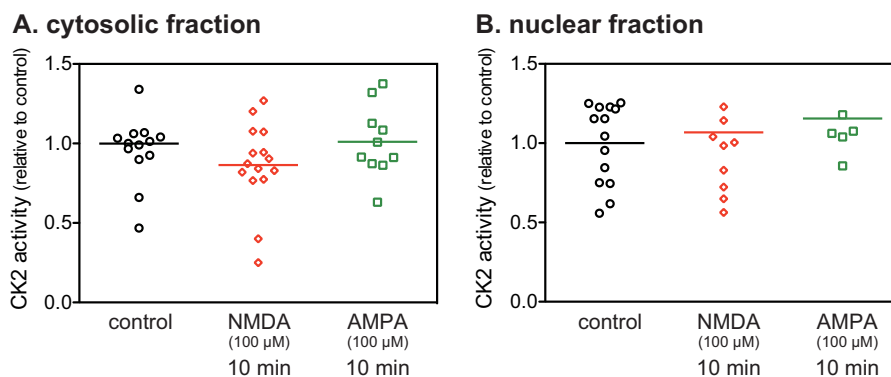
FIGURE 5. **CK2 activity in NMDA or AMPA-treated striatal slices.** CK2 activities in cytosolic (*A*) and nuclear fractions (*B*) were determined in striatal slices treated with NMDA (100 μM) or AMPA (100 μM) for 10 min. CK2 activity was normalized to that measured in control slices. Data for 6–15 experiments are presented in scatter plots with the mean values indicated.
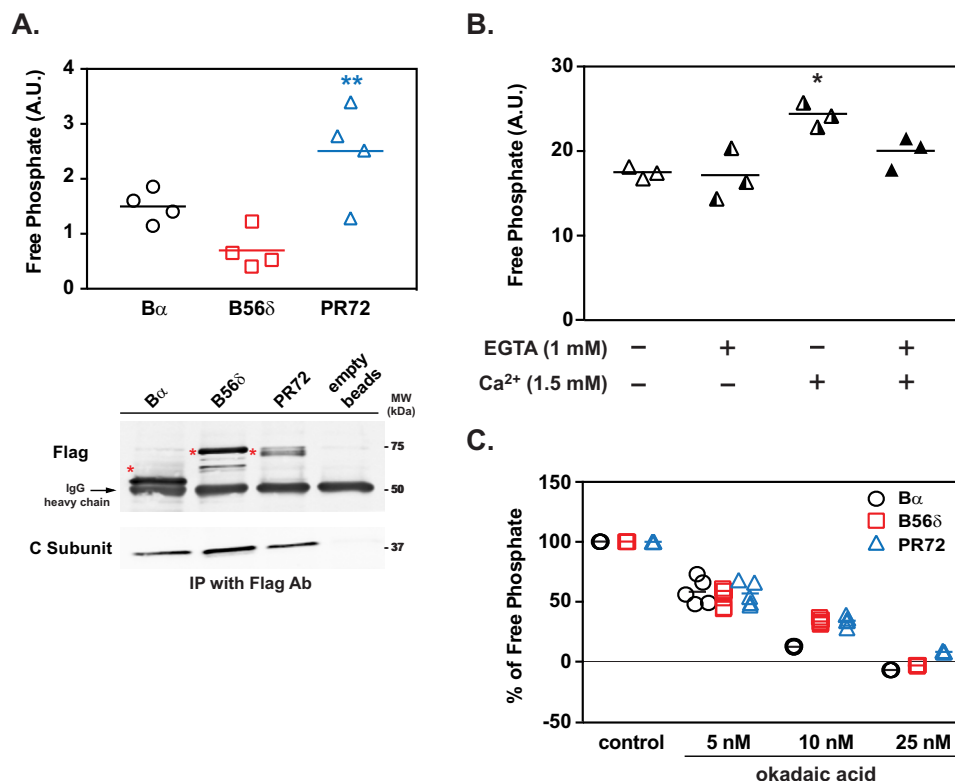
FIGURE 6. **Dephosphorylation of DARPP-32 at Ser-97 by PP2A/PR72.** *A, in vitro* phosphatase assay of PP2A heterotrimers containing either Bα, B56δ, or PR72 and using [^{32}P]Ser(P)-97-DARPP-32 as a substrate. FLAG-tagged Bα, B56δ, and PR72, immunoprecipitated as heterotrimers from lysates of HEK293 cells overexpressing individual tagged B subunits, were used for the PP2A assay. The activity of PP2A heterotrimers was normalized to the amount of the C subunit, which was measured by immunoblotting (*lower panels*). The positions of the B subunits are indicated with *asterisks*. Data for four experiments done in triplicate are presented in scatter plots with the mean values indicated. **, $p < 0.01$ compared with PP2A/B56δ, one-way ANOVA followed by Tukey's test. *B, in vitro* analysis of Ca^{2+}-dependent regulation of PP2A/PR72. Activity of PP2A-PR72 against [^{32}P]Ser(P)-97-DARPP-32 was measured in the absence or presence of Ca^{2+} (1.5 mM) and/or EGTA (1 mM). The absolute values of PP2A/PR72 activity were different from *panel A* due to different conditions of [^{32}P]Ser(P)-97-DARPP-32 and C-subunit normalization, but the values in *panels A* or *B* are uniform and comparable among treatment conditions. Data for three experiments done in triplicate are presented in scatter plots with the mean values indicated. *, $p < 0.05$ compared with untreated condition and EGTA alone, one-way ANOVA followed by Tukey's test. *C*, sensitivity of PP2A/regulatory subunit complexes to okadaic acid *in vitro* using [^{32}P]Ser(P)-97-DARPP-32 as a substrate. The ability of okadaic acid to inhibit the activity of different PP2A heterotrimers containing Bα, B56δ, or PR72 (isolated as described above) was measured. The activity of PP2A heterotrimers was normalized to the amount of C subunit for each complex, which was measured by immunoblotting. Data for five experiments done in triplicate are presented in scatter plots with the mean values indicated. *A.U.*, arbitrary units.

activated ~1.4-fold by the addition of Ca^{2+} (1.5 mM), and the Ca^{2+}-induced activation of PP2A was prevented by a Ca^{2+} chelator, EGTA (Fig. 6*B*). In addition, PP2A heterotrimers containing Bα, B56δ, or PR72 showed similar sensitivity to okadaic acid (Fig. 6*C*). The *in vitro* phosphatase assay suggests that Ser-97 of DARPP-32 is a preferential substrate for PP2A/PR72, and as found previously for other specific substrates, the dephosphorylation of Ser-97 by PP2A is activated by Ca^{2+} via interaction of Ca^{2+} with PR72 subunit (18).

Glutamate Induces Nuclear Accumulation of DARPP-32 in Cultured Striatal Neurons—Because dephosphorylation of Ser-97 after activation of D1 receptor signaling has been previously shown to increase the relative nuclear distribution of DARPP-32 (10), we examined the effects of glutamate on the nuclear localization of a fluorescently tagged DARPP-32 (D32-EGFP) in dissociated striatal neurons. Treatment with glutamate (50 μM) triggered a rapid nuclear translocation of DARPP-32, showing a 3-fold increase in the percentage of neurons with DARPP-32 enriched in the nucleus (Fig. 7, *A–C*). Treatment with NMDA (100 μM) (Fig. 7, *A–C*) or AMPA (50 μM) (Fig. 7*C*) also induced nuclear accumulation of DARPP-32 after 10 min of incubation. The effects of NMDA and AMPA

were prevented by preincubation with NMDA receptor antagonists (MK801 or AP5) and an AMPA receptor antagonist (CNQX), respectively. In addition, the effect of glutamate was antagonized by MK801 plus CNQX (Fig. 7*C*). Pretreatment of neurons with the PP2A inhibitor, okadaic acid (500 nM for 40 min), abolished the nuclear accumulation of DARPP-32 induced by glutamate, AMPA or NMDA, although okadaic acid (500 nM) alone was previously shown not to affect the nuclear localization of DARPP-32 (10). Another PP2A inhibitor, fostriecin (100 nM for 40 min), also abolished the nuclear accumulation of DARPP-32 induced by glutamate and NMDA (data not shown). In addition, activation of AMPA and/or NMDA receptors by glutamate, AMPA, or NMDA did not alter the distribution of S97A-DARPP-32, a mutant form of DARPP-32 that is less actively exported from the nucleus (Fig. 7*C*) (10). These results suggest that activation of NMDA or AMPA receptors induces the nuclear accumulation of DARPP-32 likely via mechanisms involving Ser-97 dephosphorylation by PP2A.

Priming of Striatal Slices with NMDA Suppresses the PKA-dependent Phosphorylation of DARPP-32, ERK2, MSK1, and Histone H3—It is possible that glutamate-induced nuclear sequestration of dephospho-Thr-34/dephospho-Ser-97 DARPP-32
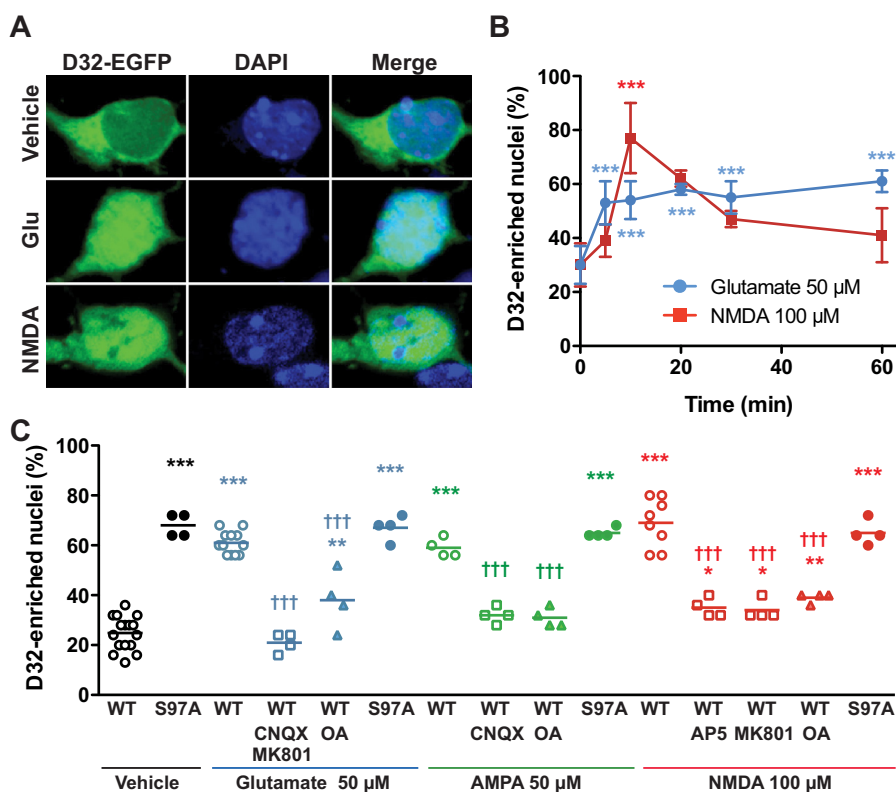
FIGURE 7. **Glutamate induces nuclear accumulation of DARPP-32 in cultured striatal neurons.** *A*, representative confocal images of striatal neurons in culture transfected with DARPP-32 fused with EGFP (*D32-EGFP*) treated for 10 min with vehicle, glutamate (*Glu*, 50 μM) or NMDA (100 μM). *B*, time course of the effects on nuclear DARPP-32, as in *A*, of glutamate (50 μM) or NMDA (100 μM) for the indicated times. Data are the means ± S.D. (*n* = 2–7 independent cultures with at least 25 transfected cells counted). One-way ANOVA: glutamate, $F_{5,16}$ = 17.02, *p* < 0.0001; NMDA, $F_{5,11}$ = 12.09, *p* = 0.0004. *C*, neurons were transfected with wild type DARPP-32-EGFP (*WT*) or D32-EGFP containing a Ser-97 to Ala mutation (*S97A*). Glutamate-induced DARPP-32 nuclear translocation was prevented by incubating striatal neurons in culture with an AMPA receptor antagonist (CNQX, 10 μM), NMDA receptor antagonists (MK801, 10 μM; AP5, 50 μM), or a PP2A inhibitor (okadaic acid (*OA*), 500 nμ) 40 min before the addition of glutamate (50 μM), AMPA (50 μM), or NMDA (100 μM) for 10 min. One-way ANOVA: $F_{14,68}$ = 53.7, *p* < 0.0001. In *B* and *C* post-hoc analysis was done with Newman-Keuls test. *, significant differences with time 0 (*B*) or WT/vehicle (*C*). †, significant differences with WT/respective agonist (glutamate or AMPA or NMDA) alone (*C*). *, *p* < 0.05; **, *p* < 0.01; *** and †††, *p* < 0.001.

interferes with PKA-mediated signaling in the cytosol and nucleus. We, therefore, examined whether prior activation of NMDA receptors affected cytosolic PKA/DARPP-32 signaling and subsequent downstream nuclear ERK/MSK1/histone H3 signaling (14). For this purpose, striatal slices were pretreated with NMDA (100 μM for 10 min), and then the PKA signaling cascade was activated by forskolin (1 μM for 60 min) (Fig. 8). NMDA pretreatment reduced the phosphorylation of DARPP-32 at Ser-97 (Fig. 8*C*) as well as at Thr-75 and Ser-130 (Fig. 8, *B* and *D*). Under this condition, forskolin/cAMP/PKA-induced phosphorylation of DARPP-32 at Thr-34, ERK2 at Thr-202/Tyr-204, MSK1 at Thr-581 and histone H3 at Ser-10 was attenuated compared with the absence of NMDA pretreatment (Fig. 8, *E–G*).

Cocaine-activated PKA Signaling Is Attenuated in the Striatum of DARPP-32 S97A Mutant Mice in Vivo—Because in DARPP-32 S97A mutant mice a large proportion of DARPP-32 is located in the nucleus of striatal neurons as compared with wild type mice (10), we hypothesized that this could impair the cytosolic function of DARPP-32 in a way that could be similar to the glutamate-primed condition that we observed in striatal slices. To test this hypothesis, we investigated two effects of acute cocaine exposure *in vivo* that have been previously shown to require DARPP-32-mediated PP1 inhibition, namely phosphorylation of GluR1 at Ser-845, a PKA site (25), and of ERK1/2

on its activation loop (26). The effects of cocaine on phosphorylation of GluR1 and ERK1/2 in striatal samples were abolished in DARPP-32 S97A mutant mice (Fig. 9, *A* and *B*). In agreement, in immunohistochemical analyses the cocaine-induced increases in the numbers of phospho-ERK-positive cells in the dorsal striatum, nucleus accumbens (NAc) core, and shell of wild type mice were also abolished in those brain regions of DARPP-32 S97 mutant mice (Fig. 9, *C–E*).

Discussion

In the present study we characterized the influence of glutamate on the phosphorylation profiles of DARPP-32 at its four major sites using different *in vitro* and *in vivo* models and its role in DARPP-32 nuclear translocation. Although previous studies have analyzed the phosphorylation/dephosphorylation of DARPP-32 in response to glutamate, this is the most comprehensive analysis to date that examines all four sites of phosphorylation under the same conditions and that compares the effect of increased glutamate and PKA signaling. Glutamate-induced Ser-97 dephosphorylation was found in both direct and indirect pathway striatal neurons. Studies in cultured striatal neurons found that glutamate increased the nuclear localization of DARPP-32 as a result of PP2A-mediated Ser-97 dephosphorylation. In striatal slices or *in vivo* in mice the dephosphorylation of Ser-97 was associated with attenuation of
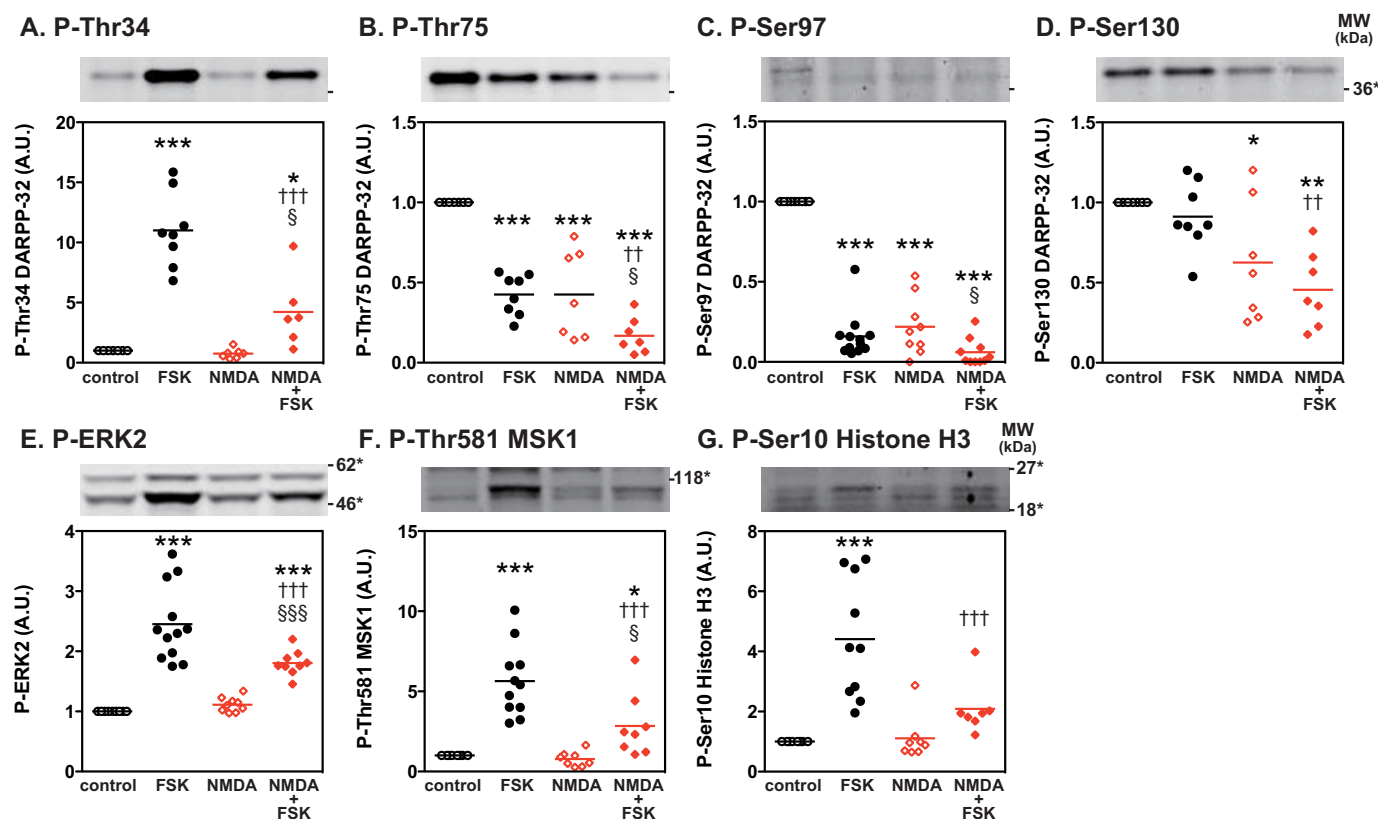
FIGURE 8. Priming effects of NMDA receptor activation on PKA/DARPP-32 and PKA/ERK/MSK1/histone H3 signaling in striatal slices. Striatal slices were pretreated with NMDA (100 μM) for 10 min and washed with Krebs-HCO$_3^-$ buffer three times followed by treatment with forskolin (1 μM) for 60 min. Changes in the phosphorylation of DARPP-32 at Thr-34 (*A*), Thr-75 (*B*), Ser-97 (*C*), and Ser-130 (*D*), ERK2 at Thr-202/Tyr-204 (the MEK sites) (*E*), MSK1 at Thr-581 (the ERK site) (*F*), and histone H3 at Ser-10 (the MSK1 site) (*G*) were determined by immunoblotting using phosphorylation state-specific antibodies. Typical immunoblots are shown at the *top of each figure*. Data for 6–12 experiments are presented in scatter plots with the mean values indicated. *, $p < 0.05$; **, $p < 0.01$; ***, $p < 0.001$ compared with control slices; ††, $p < 0.01$; †††. $p < 0.001$ compared with forskolin alone; §, $p < 0.05$; §§§, $p < 0.001$ compared with NMDA alone; one-way ANOVA followed by Newman-Keuls test. *A.U.*, arbitrary units.

PKA-dependent DARPP-32 signaling. Taken together, the results suggest that glutamate may under certain conditions counteract dopamine/D1 receptor/PKA signaling by a variety of mechanisms including nuclear sequestration of DARPP-32.

Profiles of DARPP-32 Phosphorylation; Comparison of PKA and Glutamate Signaling—Under basal conditions, DARPP-32 phosphorylation at Thr-34 is kept low with an effective stoichiometry of 0.5–1.0% in striatal neurons (12), whereas the stoichiometry of other sites: Thr-75 (~26%) (5), Ser-130 (17–33%) (27), and presumably Ser-97 (8) are relatively high (Fig. 10*A*). With such a pattern of DARPP-32 phosphorylation, the ability of DARPP-32 to inhibit PP1 is low. When dopamine D1 receptor/PKA signaling is activated, DARPP-32 is phosphorylated at Thr-34 by PKA and dephosphorylated at Thr-75 and Ser-97 by PKA-activated PP2A/B56δ (6, 18) (Fig. 10, *A* and *B*). The phosphorylation of Thr-34 (inhibition of PP1) and dephosphorylation of Thr-75 (disinhibition of PKA) have been shown to synergistically increase the phosphorylation of PKA/PP1 substrates (6). In addition, dephosphorylation of Ser-97 increases the presence of phospho-Thr-34 in the nucleus and facilitates inhibition of nuclear PP1 (10) (Fig. 10*B*). Phospho-Ser-130 DARPP-32 appears not to be a substrate for PP2A/B56δ, and presumably nuclear DARPP-32 remains phosphorylated at Ser-130 (Fig. 10*B*).

As found in the current study as well as in previous studies (12, 13, 15, 19), glutamate induced the dephosphorylation of all four sites in DARPP-32 via activation of NMDA and AMPA receptors (Fig. 10*A*). Thr-34 dephosphorylation is mediated by calcineurin (15, 28) and Thr-75 (19), and Ser-97 dephosphorylation is mediated by PP2A. *In vitro* phosphatase assays revealed that PP2A/PR72 dephosphorylated Ser-97 as well as Thr-75 (18) in a Ca^{2+}-dependent manner. Because CK2 activity was not modulated by NMDA or AMPA receptor activation, the heterotrimeric form of PP2A containing PR72 is likely to be the main regulator of glutamate-induced Ser-97 dephosphorylation (Fig. 10, *A* and *B*). Regarding Ser-130, results from studies using striatal slices suggest that Ser-130 may also be a substrate for PP2A/PR72.

Activation of NMDA and AMPA receptors induced the dephosphorylation of DARPP-32 at Thr-75, Ser-97, and Ser-130 similarly in striatonigral and striatopallidal neurons, suggesting that activation of PP2A/PR72 by glutamate is comparable between striatonigral and striatopallidal neurons. The smaller effects of NMDA and AMPA receptors on Thr-34 dephosphorylation in striatonigral neurons suggest differential regulation of calcineurin in the two types of neurons. Because the expression levels of calcineurin mRNA are similar in striatonigral and striatopallidal neurons (29), it is possible that calcineurin in
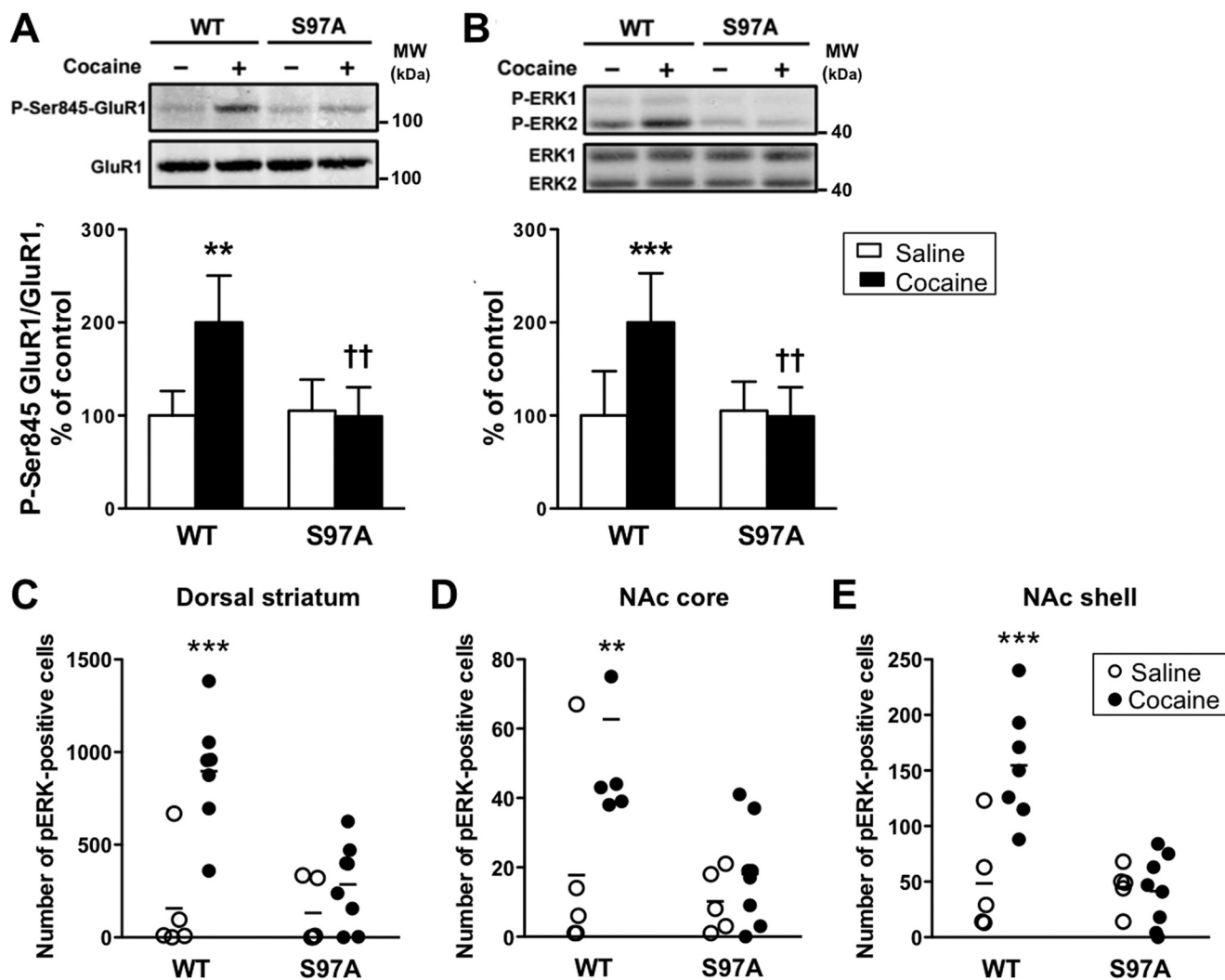
FIGURE 9. **Cocaine-induced GluR1 and ERK phosphorylation in the striatum of DARPP-32 S97A mutant mice *in vivo*.** *A* and *B*, WT and S97A mice were injected with saline ($-$, *open bars*) or cocaine 20 mg/kg ($+$, *closed bars*) and killed 10 min later. Frozen tissue from the dorsal striatum was used for phosphorylation analyses. *A*, phospho-Ser-845 (*P-Ser-845-GluR1, upper panel*) and total (*lower panel*) GluR1 were analyzed by immunoblotting. Results are expressed as ratios of phosphorylated/total protein and normalized to the mean of saline-treated wild type mice. Data for 5–7 mice per group represent the means $\pm$ S.D. and were analyzed using two-way ANOVA: interaction between genotype and treatment, $F_{1,20} = 4.44$, $p < 0.05$; effect of treatment, $F_{1,20} = 6.55$, $p < 0.05$; effect of genotype $F_{1,20} = 9.08$, $p < 0.01$. *B*, same as in *A* except that phospho-ERK1/2 (*P-ERK1, P-ERK2, upper panel*) and total ERK1 and ERK2 (*lower panel*) were studied. Because P-ERK1 was barely detectable in most experiments, only P-ERK2 has been quantified. Data for 5–7 mice per group represent the means $\pm$ S.D. and were analyzed using two-way ANOVA; interaction between genotype and treatment, $F_{1,20} = 8.57$, $p < 0.01$; effect of treatment, $F_{1,20} = 6.74$, $p < 0.05$; effect of genotype $F_{1,20} = 7.03$, $p < 0.05$. Bonferroni post-test: **, $p < 0.01$; ***, $p < 0.001$ cocaine *versus* saline; ††, $p < 0.01$ S97A *versus* WT. *C–E*, immunohistochemical analysis of P-ERK in the dorsal striatum (*C*), NAc core (*D*), and NAc shell (*E*) from wild type and S97A mice. WT and S97A mice were injected with saline (*open bars*) or cocaine 20 mg/kg (*closed bars*) and killed 15 min later. Numbers of P-ERK-positive cells above background were counted. Data (5–7 mice per group) were analyzed using two-way ANOVA. Dorsal striatum: interaction between genotype and treatment, $F_{1,21} = 7.66$, $p < 0.05$; effect of treatment, $F_{1,21} = 17.78$, $p < 0.001$; effect of genotype $F_{1,21} = 8.96$, $p < 0.01$. Bonferroni post-test: ***$p < 0.001$ cocaine *versus* saline. *NAc core*: interaction between genotype and treatment, $F_{1,21} = 4.16$, $p = 0.054$; effect of treatment, $F_{1,21} = 8.49$, $p < 0.01$; effect of genotype $F_{1,21} = 8.29$, $p < 0.01$. Bonferroni post-test: **, $p < 0.01$ cocaine *versus* saline. *NAc shell*: interaction between genotype and treatment, $F_{1,21} = 11.45$, $p < 0.01$; effect of treatment, $F_{1,21} = 10.04$, $p < 0.01$; effect of genotype $F_{1,21} = 12.92$, $p < 0.01$; Bonferroni post-test: ***, $p < 0.001$ cocaine *versus* saline.

striatonigral neurons may be active under basal conditions to keep Thr-34 phosphorylation low, and therefore, the extent of glutamate-induced activation of calcineurin may be more limited in striatonigral neurons.

Glutamate-induced Nuclear Localization of Inactive DARPP-32 via Dephosphorylation of Ser-97—Phosphorylation of DARPP-32 by CK2 has pleiotropic effects on its properties. Initial studies of the phosphorylation of DARPP-32 by CK2 supported its role in facilitation of the phosphorylation of DARPP-32 at Thr-34 by PKA (8). Subsequent studies revealed that Ser-97 phosphorylation of DARPP-32 acts in conjunction

with a nuclear export signal to facilitate export of DARPP-32 from the nucleus (10). In addition, phosphorylation of Ser-97 increases the interaction of DARPP-32 with adducin, a protein associated with cortical actin-spectrin cytoskeleton (11). The results from the current study suggest that glutamate can act via AMPA and/or NMDA receptors to induce the dephosphorylation of DARPP-32 at Ser-97 by PP2A/PR72. This is expected to alter DARPP-32-mediated signaling by opposing all of the effects of phospho-Ser-97. One effect supported by the present study is the accumulation of DARPP-32 in the nucleus of striatal neurons, possibly by impairment of the nuclear export
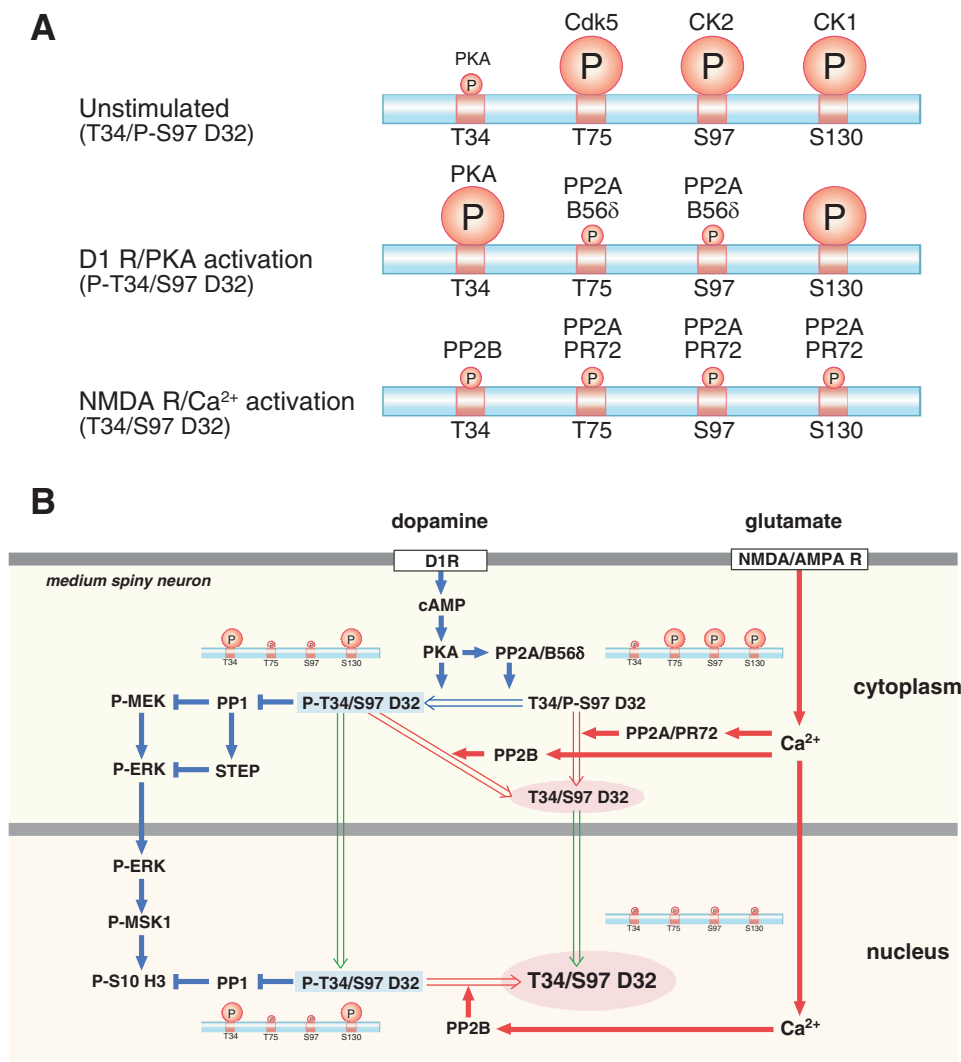
FIGURE 10. **Schemes showing the regulation of DARPP-32 phosphorylation and nuclear translocation by dopamine D1 receptor/PKA and glutamate/NMDA and AMPA receptor (*AMPAR*)/Ca²⁺ signaling.** *A*, DARPP-32 phosphorylation patterns under unstimulated, dopamine D1 receptor (D1R)/PKA-activated, and NMDA/AMPA receptor/Ca²⁺-activated conditions. The relative levels of phosphorylation of Thr-34 (*T34*), Thr-75 (*T75*), Ser-97 (*S97*), and Ser-130 (*S130*) are indicated by the size of the *circled P*. *B*, *right side of figure illustrated with blue arrows*, activation of dopamine D1 receptor/PKA signaling induces DARPP-32 Thr-34 phosphorylation and DARPP-32 dephosphorylation at Thr-75 and Ser-97 by PP2A/B56δ. *Left side of figure illustrated with red arrows*, activation of NMDA or AMPA receptors followed by an increase in intracellular Ca²⁺ induces DARPP-32 dephosphorylation at all four sites: Thr-34 dephosphorylation by calcineurin (PP2B); Thr-75, Ser-97, and Ser-130 dephosphorylation by PP2A/PR72. PKA and Ca²⁺ signals induce Ser-97 dephosphorylation via different mechanisms of PP2A activation, leading to the nuclear accumulation of different forms of DARPP-32 (*green arrows*). After D1 dopamine receptor stimulation and activation of PKA, DARPP-32 phosphorylated at Thr-34 translocates to the nucleus where it retains the ability to inhibit PP1 and potentiate dopamine signaling. After glutamate receptor activation, DARPP-32 translocates to the nucleus in a form where Thr-34 is in the dephosphorylated state and thus unable to inhibit PP1.

mechanism (10) and also by decreased binding to adducin, which is a cytoplasmic partner (11). However, in contrast to the nuclear accumulation of phospho-Thr-34 DARPP-32 observed after activation of PKA signaling, following glutamate signaling, dephospho-Thr-34 DARPP-32 accumulates in the nucleus (Fig. 10*B*). This would result in a shift of DARPP-32 away from its cytoplasmic effects and contribute to alteration of signaling responses. However, it should be pointed out that the PKA catalytic subunit, when released from the regulatory subunit after cAMP binding can move to the nucleus and phosphorylate substrates including DARPP-32 (30–32). Thus, it is likely that a shift in the cytonuclear distribution of DARPP-32 alters the kinetics of phosphorylation by PKA by increasing its distance from PKA activated in dendrite. It is also predicted to impair

phospho-Thr-34 DARPP-32 to inhibit PP1 in perinuclear cytoplasm and dendrites rather than completely block its signaling. In support of this model, priming of striatal neurons with NMDA receptor activation attenuated the effects of PKA activation to phosphorylate DARPP-32 at Thr-34 and to increase phosphorylation of ERK2 and its downstream nuclear targets such as MSK1 and histone H3. The ability of cocaine to induce the phosphorylation of GluR1 and ERK2 via activation of dopamine/D1 receptor/PKA signaling in striatal neurons *in vivo* (25, 26) was also lost in DARPP-32 S97A mutant mice. In behavioral analyses, DARPP-32 S97A mutant mice exhibited reduced responses to the rewarding effects of drugs of abuse and reduced motivation for food reward (10). As the S97A mutation mimics the effect of NMDA receptor activation on

Ser-97, we can speculate that the priming with glutamate may attenuate the responses to drugs of abuse and natural rewarding stimuli. Alternatively, it is also possible that strong corticostriatal or thalamostriatal glutamatergic inputs inactivate DARPP-32 function to avoid enhancement of glutamatergic signaling by dopamine D1 receptors. In addition to the contribution of changes in the cytonuclear distribution of DARPP-32, it is likely that the loss of the facilitatory effect of CK2 phosphorylation of DARPP-32 on phosphorylation of Thr-34 by PKA (8) may also contribute to the impairment of signaling.

In summary, taken together with previous observations, the current study emphasizes the complex role played by glutamate in the regulation of DARPP-32 and its subsequent influence on signaling in striatal neurons. The results in the current study suggest that glutamate can regulate DARPP-32 phosphorylation at Ser-97 and thereby decrease its responsiveness to cAMP/PKA, possibly directly and by sequestering it in the nucleus. Activation of glutamate signaling has also been shown to counteract the PKA-dependent phosphorylation of DARPP-32 at Thr-34 by activation of calcineurin-mediated dephosphorylation (12, 13). In contrast, coincident activation of D1 dopamine receptors and NMDA glutamate receptors have been shown to have a synergistic effect in striatal neurons that results in potentiation of ERK activation and subsequent downstream signaling (33). The precise pattern of the response to coincident or non-coincident glutamate and dopamine signals may utilize the control of DARPP-32 cytoplasmic and nuclear translocation to effect positive or negative signaling. Because the same stimuli, dopamine and glutamate, can have synergistic or antagonistic effects depending on their relative timing and intensity, we suggest that their combination and integration by intracellular signaling pathways such as DARPP-32, plays an important role in shaping the timing-sensitivity of striatal neuron plasticity (34, 35).

Experimental Procedures

Preparation and Incubation of Neostriatal Slices—Male C57BL/6 mice at 6–8 weeks old were purchased from Japan SLC (Shizuoka, Japan). All mice used to generate striatal slices were handled in accordance with the Guide for the Care and Use of Laboratory Animals as adopted and promulgated by the United States National Institutes of Health. The specific protocols were approved by the Institutional Animal Care and Use Committee of Kurume University School of Medicine. Male C57BL/6 mice were sacrificed by decapitation. The brains were rapidly removed and placed in ice-cold, oxygenated Krebs-HCO_3^- buffer (124 mM NaCl, 4 mM KCl, 26 mM NaHCO$_3$, 1.5 mM CaCl$_2$, 1.25 mM KH$_2$PO$_4$, 1.5 mM MgSO$_4$, and 10 mM D-glucose, pH 7.4). Coronal slices (350 μm) were prepared using a vibrating blade microtome, VT1000S (Leica Microsystems, Nussloch, Germany) as described previously (15). From each mouse, six slices of the dorsal striatum (striatal slices) were dissected from the coronal slices in ice-cold Krebs-HCO_3^- buffer. Each slice was placed in a polypropylene incubation tube with 2 ml of fresh Krebs-HCO_3^- buffer containing adenosine deaminase (10 μg/ml). The slices were preincubated at 30 °C under constant oxygenation with 95% O$_2$, 5% CO$_2$ for 60 min. The buffer was replaced with fresh Krebs-HCO_3^- buffer after 30

min of preincubation. Each slice was treated with drugs as specified in each experiment. Drugs were obtained from the following sources: AMPA, CNQX, forskolin, glutamate, MK801, and NMDA from Sigma; LY367385, MPEP, and okadaic acid from Tocris Cookson (Bristol, UK). After drug treatment slices were transferred to Eppendorf tubes, frozen on dry ice, and stored at −80 °C until assayed.

Frozen tissue samples were sonicated in boiling 1% sodium dodecyl sulfate (SDS) and boiled for an additional 10 min. Small aliquots of the homogenate were retained for protein determination by the BCA protein assay method (Pierce). Equal amounts of protein (40 μg) were loaded onto 10% polyacrylamide gels or 4–12% polyacrylamide Bis-Tris gels (#345-0124; Bio-Rad), separated by electrophoresis, and transferred to nitrocellulose membranes (0.2 μm) (Schleicher & Schüll). When samples were separated using 4–12% polyacrylamide Bis-Tris gels, proteins migrated differently from their actual molecular weights. In these cases, molecular weight markers are indicated with *asterisks* in immunoblots.

Immunoprecipitations of FLAG- and Myc-tagged DARPP-32 in Striatal Slices from D1-DARPP-32-FLAG/D2-DARPP-32-Myc Mice—D$_1$-DARPP-32-FLAG/D$_2$-DARPP-32-Myc transgenic mice express FLAG- and Myc-tagged DARPP-32 under the control of dopamine D1 and D2 receptor promoters, respectively (22). In the striatum, FLAG-tagged DARPP-32 was shown to be expressed selectively in D1 receptor-enriched striatonigral neurons, and Myc-tagged DARPP-32 was shown to be expressed selectively in D2 receptor-enriched striatopallidal neurons. Using antibodies against either FLAG or Myc, DARPP-32 was selectively immunoprecipitated from D1 receptor- or D2 receptor-expressing neurons, and the phosphorylation state of DARPP-32 was analyzed in a neuronal type-specific manner. For each of 3 treatment conditions, 6 slices were collected from 3 mice (2 slices from each mouse, 18 slices total). The six slices of the dorsal striatum from each treatment condition were pooled as one sample for the analysis of DARPP-32 phosphorylation. The three sets of pooled slices were sonicated in 720 μl of immunoprecipitation (IP) lysis buffer (50 mM Tris-HCl, pH 7.5, 150 mM NaCl, 1 mM EDTA, 1% Triton X-100, 1% SDS, 100 nM okadaic acid, phosphatase inhibitor mixture (#P5726; Sigma), and protease inhibitor mixture (#11873580001; Roche Applied Science). After determination of protein concentration, 15 μg of protein was saved for the analysis of DARPP-32 phosphorylation in total striatal homogenate, and the residual homogenates were used for IP. For each IP from striatal homogenate, 50 μl of washed EZView Red anti-FLAG M2 affinity gel (Sigma) and 45 μl of anti-Myc antibody (Novus Biologicals, Littleton, CO) coupled to magnetic beads (3 μg of Myc antibody for every 5 μl of magnetic beads) (Dynabeads M-280 Tosyl-activated; Invitrogen) were added. The homogenate/antibody mixture was gently rotated overnight at 4 °C. After the overnight incubation, the Myc magnetic beads were separated from the homogenate/antibody mixture using a magnetic particle concentrator (Invitrogen), and then the FLAG affinity gels were separated by centrifugation. The Myc magnetic beads and FLAG affinity gels were washed with 1× PBS 3 times. After the final wash, 30 μl of sample buffer was added, and samples were boiled for 2 min.

FLAG IP, Myc IP, and total striatal samples were loaded onto 4–12% polyacrylamide Bis-Tris gels (Bio-Rad), separated by electrophoresis, and transferred to nitrocellulose membranes (0.2 μM) (Schleicher & Schüll).

Preparation of Striatal Tissues for Analysis of Protein Phosphorylation in Vivo—Experiments were carried out in accordance with the guidelines of the French Agriculture and Forestry Ministry for handling animals (Decree 87849, License 01499) in either 8–12-week-old male and female DARPP-32 S97A mutant mice and matched controls from previously described S97A line (36). Mice were habituated to daily saline i.p. injections during the 3 days preceding the experiments and treated with 20 mg/kg cocaine in saline as described previously (26). Fifteen minutes later mice were deeply anesthetized with pentobarbital, and their heads were immediately frozen in liquid nitrogen. The frozen brains were cut with a cryostat into 210-μm-thick slices, and 5 or 6 microdisks (diameter 1.4 mm) were punched out bilaterally from the dorsal striatum and stored at −80 °C. Microdisks were lysed by sonication in 1% (v/v) SDS containing 1 mM sodium orthovanadate at 100 °C and maintained at this temperature for 5 min to inactivate phosphatases and proteases. Equal amounts of lysates (100 μg of protein) were analyzed by immunoblotting.

Immunoblotting—Membranes were immunoblotted using phosphorylation state-specific antibodies raised against phosphopeptides: phospho-Thr-34 DARPP-32, a site phosphorylated by PKA (#CC500, 1:4000 dilution) (37); phospho-Thr-75 DARPP-32, the site phosphorylated by Cdk5 (#911, 1:2000 dilution) (5); phospho-Ser-97 DARPP-32, the site phosphorylated by CK2 (#ITI A7335, 1:500 dilution; #RU1736, 1:5000 dilution) (10, 38); phospho-Ser-130 DARPP-32, the site phosphorylated by CK1 (#RU404, 1:1000 dilution) (17); phospho-Thr-202/Tyr-204 ERK, the site phosphorylated by MEK (#9101, 1:5000 dilution) (Cell Signaling Technology, Danvers, MA); phospho-Thr-581 MSK1, the site phosphorylated by ERK (#9595, 1:500 dilution) (Cell Signaling Technology); phospho-Ser-10 histone H3, the site phosphorylated by MSK1 (#3H10, 1:500 dilution) (Upstate Biotechnology, Lake Placid, NY). Antibodies generated against DARPP-32 (#C24-5a, 1:20,000 dilution), ERK (#9102, 1:1,000 dilution) (New England BioLabs, Beverly, MA), histone H3 (#06-755, 1:500 dilution) (Upstate Biotechnology), which are not phosphorylation state-specific, were used to determine the total amount of proteins. None of the experimental manipulations used in the present study altered the total levels of specific phosphoproteins.

Membranes were incubated with a goat anti-mouse or rabbit IgG Alexa 680-coupled antibody (1:5000 dilution) (Molecular Probes, Eugene, OR) or a goat anti-mouse or rabbit IgG IRDye800-coupled antibody (1:5000 dilution) (Rockland Immunochemicals, Gilbertsville, PA). Fluorescence at infrared wavelengths was detected using an Odyssey infrared imaging system (LI-COR, Lincoln, NE), and quantified using Odyssey software. In an individual experiment, samples from control and drug-treated slices were analyzed on the same immunoblot. For each experiment, values obtained for slices were normalized to values for either the control or the drug-treated slices, as described in the figure legends. Normalized data from multiple experiments were averaged, and statistical analysis was carried out as described in the figure legends.

For analysis of protein phosphorylation *in vivo*, the following antibodies were used: mouse monoclonal antibodies for phospho-Thr/Tyr ERK1/2 (clone MAPK-YT, 1:1000, Sigma), ERK1/2 (#06-182, 1:1000) (Upstate Biotechnology); rabbit polyclonal antibodies against phospho-Ser-845 GluR1 (#06-773, 1:500) (Upstate Biotechnology), GluR1 (#06-306, 1:500) (Upstate Biotechnology). Bound antibodies were detected with anti-rabbit IgG IRdye800CW-coupled and anti-mouse IgG IRdye700DX-coupled antibodies (Rockland Immunochemicals) and the Odyssey infrared imaging system (LI-COR). Data were normalized to the mean value of untreated controls in the same gels.

Immunohistochemical Analysis of ERK Phosphorylation—Immunohistochemical analysis was performed as described previously (26). Fifteen minutes after cocaine (20 mg/kg, i.p.) administration, the animals were rapidly anesthetized with pentobarbital (500 mg/kg, i.p.; Sanofi-Aventis, Paris, France) and perfused transcardially with a fixative solution containing 4% paraformaldehyde (w/v) in PBS, pH 7.5. Brains were postfixed overnight in the same solution and stored at 4 °C. Sections (30 μm thick) were cut with a vibratome (Leica) and kept at −20 °C in a solution containing 30% ethylene glycol (v/v), 30% glycerol (v/v), and 0.1 M phosphate buffer. For detection of phosphorylated proteins, 50 mM NaF was included in all buffers and incubation solutions. Active ERK was detected with rabbit polyclonal antibodies against phospho-Thr-202/Tyr-204-ERK1/2 (1:400; Cell Signaling Technology), and immunolabeling was performed using Alexa 488-coupled secondary antibody (Invitrogen). Images were captured using sequential laser scanning confocal microscopy (SP2; Leica) and analyzed using Meta-Morph software (Universal Imaging, Downingtown, PA). Quantification was performed by counting the number of cells with nuclear fluorescence above background using a MetaMorph analyzer in two brain sections per animal in the dorsal striatum and NAc shell and core.

Nuclear Localization of EGFP-tagged DARPP-32 in Cultured Striatal Neurons—Cultures were prepared as described (10, 39). Striata were dissected out from 14-day Swiss mouse embryos (Janvier Labs, Le Genest-Saint-Isle, France) and mechanically dissociated by gently pipetting in modified L-15 medium. After decantation for 10 min at room temperature to eliminate tissue debris, cells were collected by centrifugation at 1000 × g for 5 min. Cell pellets were suspended in Neurobasal medium (B27 supplement (Invitrogen), 500 nM L-glutamine, 60 μg/ml penicillin G, 25 μM 2-mercaptoethanol) and then plated onto coverslips (180,000 per well) precoated with 10 μg/ml poly-D-lysine (Sigma). Cells were seeded in the Neurobasal medium and cultured at 37 °C in a humidified atmosphere of 95% air and 5% CO_2. Cells were transfected after 7 days in culture with DARPP-32-EGFP (1 mg) DNA using Lipofectamine 2000 in Opti-MEM serum-free medium. Treatments were done 24 h later in fresh Neurobasal medium and immediately after cells fixed with PBS containing 2% paraformaldehyde (40 min, 20–23 °C). Nuclei were counterstained with DAPI. Cells rinsed three times were mounted under coverslips with Vectashield (Vector Laboratories). The subcellular localization

of DARPP-32-EGFP was analyzed with a sequential laser scanning confocal microscope (SP2; Leica). Green fluorescence was visualized with a 488-nm laser, and images of individual transfected neurons were acquired (>25 neurons per coverslip, $n = 4-16$ coverslips/experimental condition). The proportion of neurons with DARPP-32-EGFP-enriched nuclei was determined based on the difference of EGFP intensity levels between the nucleus and the somatic cytoplasm as performed previously (10). DARPP-32-EGFP was scored as localizing to the nucleus if the fluorescence signal in the cytoplasm was weaker or equal to the nuclear staining. Values for each coverslip were averaged for statistical analysis.

Measurement of CK2 Activity in Striatal Slices after AMPA/NMDA Treatment—Striatal slices were prepared and preincubated as described above. Treatment of slices with AMPA and NMDA was performed as indicated, and slices were immediately snap-frozen thereafter. Slices were then homogenized in homogenization buffer (15 mM Tris-HCl, pH 7.9, 5 mM KCl, 0.5 mM $MgCl_2$, 0.05 mM EDTA, 0.5 mM DTT, 0.05% Triton X-100, 350 mM sucrose plus protease inhibitor mixture (Roche Applied Science)) by 10 strokes through a 22-gauge syringe. Lysates were centrifuged at low speed (800 × g) for 3 min at 4 °C. The supernatant was ultracentrifuged (100,000 × g, 1 h, 4 °C), and the resulting supernatant was considered as the cytosolic fraction. The nuclear pellet from the initial centrifugation was washed once and re-centrifuged at 800 × g for 3 min. The pellet was then resuspended in extraction buffer (20 mM HEPES, 400 mM NaCl, 1 mM EDTA, 1 mM DTT, plus protease inhibitor mixture), extracted for 30 min at 4 °C, and centrifuged (20,000 × g, 20 min). The resulting supernatants were designated as nuclear extracts. BCA protein quantification was performed, and 10 μg of lysate was added to phosphorylation buffer containing 50 mM Tris-HCl, pH 8.2, 50 mM $NaCl_2$, 25 mM KCl, 10 mM $MgCl_2$, 10 μM sodium orthovanadate, 2 μM PKA inhibitor mixture (Upstate Biotechnology), 100 μM ATP, 5 μCi of [γ-^{32}P]ATP, and 150 μM CK2 substrate peptide (Upstate Biotechnology). Total volume was 50 μl per sample. Reactions were incubated at 30 °C for 10 min and stopped by the addition of 8 μl of trichloroacetic acid (TCA). Reaction mixes were spotted onto P81 Whatman paper and washed 5× in 0.5% phosphoric acid, 2× in 95% ethanol and air-dried. Phosphorylation was quantified using a Beckmann scintillation counter. A control assay that did not contain any substrate peptide was used to subtract non-CK2-dependent baseline phosphorylation. It has been shown that the CK2 substrate peptide is phosphorylated by CK2 but not by other protein kinases including CK1 (40 – 42), indicating that the CK2 substrate peptide is very specific for CK2.

Dephosphorylation of Ser(P)-97 DARPP-32 by a PP2A Heterotrimer Containing Bα, B56δ, or PR72—Recombinant purified DARPP-32 was phosphorylated by CK2 at 30 °C for 30 min with 200 μM [γ-^{32}P]ATP. Proteins were precipitated by the addition of 100% TCA, and the pellet was resuspended and dialyzed in 20 mM Tris-HCl, pH 7.6, 5 mM β-mercaptoethanol. For the PP2A assay, different PP2A heterotrimers (Bα, B56δ, and PR72), which were isolated by immunoprecipitation with a FLAG antibody (#F1804; Sigma) from HEK293 cells transfected with FLAG-tagged Bα, B56δ, or PR72 (7, 18), were incubated with 37.5 μM [^{32}P]Ser(P)-97-DARPP-32 for 10 min at 30 °C (buffer: 20 mM Tris-HCl, pH 7.6, 5 mM β-mercaptoethanol, BSA 1 mg/ml). Free ^{32}P was measured by Cerenkov radiation counting after precipitation of [^{32}P]phosphoproteins with cold TCA. The values of free ^{32}P obtained for the different PP2A heterotrimers were normalized for the amount of C subunit immunoprecipitated in each complex, quantified by immunoblot analyses using antibodies for PP2A C subunit (#05-421, 1:2000 dilution) (Millipore Corp., Bedford, MA) and FLAG (#F1804, 1:1000 dilution) (Sigma), the anti-mouse IgG IRDye800CW-coupled antibody (Rockland Immunochemicals), and the Odyssey infrared imaging system (LI-COR).

References

1. Greengard, P., Allen, P. B., and Nairn, A. C. (1999) Beyond the dopamine receptor: the DARPP-32/protein phosphatase-1 cascade. *Neuron* **23,** 435–447
2. Svenningsson, P., Nishi, A., Fisone, G., Girault, J. A., Nairn, A. C., and Greengard, P. (2004) DARPP-32: an integrator of neurotransmission. *Annu. Rev. Pharmacol. Toxicol.* **44,** 269–296
3. Walaas, S. I., Hemmings, H. C., Jr, Greengard, P., and Nairn, A. C. (2011) Beyond the dopamine receptor: regulation and roles of serine/threonine protein phosphatases. *Front. Neuroanat.* **5,** 50
4. Yger, M., and Girault, J. A. (2011) DARPP-32, Jack of All Trades. Master of Which? *Front. Behav. Neurosci.* **5,** 56
5. Bibb, J. A., Snyder, G. L., Nishi, A., Yan, Z., Meijer, L., Fienberg, A. A., Tsai, L. H., Kwon, Y. T., Girault, J. A., Czernik, A. J., Huganir, R. L., Hemmings, H. C., Jr, Nairn, A. C., and Greengard, P. (1999) Phosphorylation of DARPP-32 by Cdk5 modulates dopamine signalling in neurons. *Nature* **402,** 669–671
6. Nishi, A., Bibb, J. A., Snyder, G. L., Higashi, H., Nairn, A. C., and Greengard, P. (2000) Amplification of dopaminergic signaling by a positive feedback loop. *Proc. Natl. Acad. Sci. U.S.A.* **97,** 12840–12845
7. Ahn, J. H., McAvoy, T., Rakhilin, S. V., Nishi, A., Greengard, P., and Nairn, A. C. (2007) Protein kinase A activates protein phosphatase 2A by phosphorylation of the B56δ subunit. *Proc. Natl. Acad. Sci. U.S.A.* **104,** 2979–2984
8. Girault, J.-A., Hemmings, H. C., Jr., Williams, K. R., Nairn, A. C., and Greengard, P. (1989) Phosphorylation of DARPP-32, a dopamine- and cAMP-regulated phosphorprotein, by casein kinase II. *J. Biol. Chem.* **264,** 21748–21759
9. Desdouits, F., Siciliano, J. C., Greengard, P., and Girault, J.-A. (1995) Dopamine- and cAMP-regulated phosphoprotein DARPP-32: phosphorylation of Ser-137 by casein kinase I inhibits dephosphorylation of Thr-34 by calcineurin. *Proc. Natl. Acad. Sci., U.S.A.* **92,** 2682–2685
10. Stipanovich, A., Valjent, E., Matamales, M., Nishi, A., Ahn, J. H., Maroteaux, M., Bertran-Gonzalez, J., Brami-Cherrier, K., Enslen, H., Corbillé, A. G., Filhol, O., Nairn, A. C., Greengard, P., Hervé, D., and Girault, J. A. (2008) A phosphatase cascade by which rewarding stimuli control nucleosomal response. *Nature* **453,** 879–884

11. Engmann, O., Giralt, A., Gervasi, N., Marion-Poll, L., Gasmi, L., Filhol, O., Picciotto, M. R., Gilligan, D., Greengard, P., Nairn, A. C., Hervé, D., and Girault, J. A. (2015) DARPP-32 interaction with adducin may mediate rapid environmental effects on striatal neurons. *Nat. Commun.* **6,** 10099

12. Nishi, A., Snyder, G. L., and Greengard, P. (1997) Bidirectional regulation of DARPP-32 phosphorylation by dopamine. *J. Neurosci.* **17,** 8147–8155

13. Halpain, S., Girault, J.-A., and Greengard, P. (1990) Activation of NMDA receptors induced dephosphorylation of DARPP-32 in rat striatal slices. *Nature* **343,** 369–372

14. Girault, J. A., Valjent, E., Caboche, J., and Hervé, D. (2007) ERK2: a logical AND gate critical for drug-induced plasticity? *Curr. Opin. Pharmacol.* **7,** 77–85

15. Nishi, A., Watanabe, Y., Higashi, H., Tanaka, M., Nairn, A. C., and Greengard, P. (2005) Glutamate regulation of DARPP-32 phosphorylation in neostriatal neurons involves activation of multiple signaling cascades. *Proc. Natl. Acad. Sci. U.S.A.* **102,** 1199–1204

16. Nishi, A., Liu, F., Matsuyama, S., Hamada, M., Higashi, H., Nairn, A. C., and Greengard, P. (2003) Metabotropic mGlu5 receptors regulate adenosine A2A receptor signaling. *Proc. Natl. Acad. Sci. U.S.A.* **100,** 1322–1327

17. Liu, F., Ma, X. H., Ule, J., Bibb, J. A., Nishi, A., DeMaggio, A. J., Yan, Z., Nairn, A. C., and Greengard, P. (2001) Regulation of cyclin-dependent kinase 5 and casein kinase 1 by metabotropic glutamate receptors. *Proc. Natl. Acad. Sci. U.S.A.* **98,** 11062–11068

18. Ahn, J. H., Sung, J. Y., McAvoy, T., Nishi, A., Janssens, V., Goris, J., Greengard, P., and Nairn, A. C. (2007) The B''/PR72 subunit mediates Ca^{2+}-dependent dephosphorylation of DARPP-32 by protein phosphatase 2A. *Proc. Natl. Acad. Sci. U.S.A.* **104,** 9876–9881

19. Nishi, A., Bibb, J. A., Matsuyama, S., Hamada, M., Higashi, H., Nairn, A. C., and Greengard, P. (2002) Regulation of DARPP-32 dephosphorylation at PKA- and Cdk5-sites by NMDA and AMPA receptors: distinct roles of calcineurin and protein phosphatase-2A. *J. Neurochem.* **81,** 832–841

20. Tanda, K., Nishi, A., Matsuo, N., Nakanishi, K., Yamasaki, N., Sugimoto, T., Toyama, K., Takao, K., and Miyakawa, T. (2009) Abnormal social behavior, hyperactivity, impaired remote spatial memory, and increased D1-mediated dopaminergic signaling in neuronal nitric oxide synthase knock-out mice. *Mol. Brain.* **2,** 19

21. Desdouits, F., Siciliano, J. C., Nairn, A. C., Greengard, P., and Girault, J. A. (1998) Dephosphorylation of Ser-137 in DARPP-32 by protein phosphatases 2A and 2C: different roles *in vitro* and in striatonigral neurons. *Biochem. J.* **330,** 211–216

22. Bateup, H. S., Svenningsson, P., Kuroiwa, M., Gong, S., Nishi, A., Heintz, N., and Greengard, P. (2008) Cell type-specific regulation of DARPP-32 phosphorylation by psychostimulant and antipsychotic drugs. *Nat. Neurosci.* **11,** 932–939

23. Bertran-Gonzalez, J., Bosch, C., Maroteaux, M., Matamales, M., Hervé, D., Valjent, E., and Girault, J. A. (2008) Opposing patterns of signaling activation in dopamine D1 and D2 receptor-expressing striatal neurons in response to cocaine and haloperidol. *J. Neurosci.* **28,** 5671–5685

24. Girault, J.-A., Hemmings, H. C., Jr., Zorn, S. H., Gustafson, E. L., and Greengard, P. (1990) Characterization in mammalian brain of a DARPP-32 serine kinase identical to casein kinase II. *J. Neurochem.* **55,** 1772–1783

25. Snyder, G. L., Allen, P. B., Fienberg, A. A., Valle, C. G., Huganir, R. L., Nairn, A. C., and Greengard, P. (2000) Regulation of phosphorylation of the GluR1 AMPA receptor in the neostriatum by dopamine and psychostimulants *in vivo. J. Neurosci.* **20,** 4480–4488

26. Valjent, E., Pascoli, V., Svenningsson, P., Paul, S., Enslen, H., Corvol, J. C., Stipanovich, A., Caboche, J., Lombroso, P. J., Nairn, A. C., Greengard, P., Hervé, D., and Girault, J. A. (2005) Regulation of a protein phosphatase cascade allows convergent dopamine and glutamate signals to activate ERK in the striatum. *Proc. Natl. Acad. Sci. U.S.A.* **102,** 491–496

27. Desdouits, F., Cohen, D., Nairn, A. C., Greengard, P., and Girault, J.-A. (1995) Phosphorylation of DARPP-32, a dopamine- and cAMP-regulated phosphoprotein, by casein kinase I *in vitro* and *in vivo. J. Biol. Chem.* **270,** 8772–8778

28. Nishi, A., Snyder, G. L., Nairn, A. C., and Greengard, P. (1999) Role of calcineurin and protein phosphatase-2A in the regulation of DARPP-32 dephosphorylation in neostriatal neurons. *J. Neurochem.* **72,** 2015–2021

29. Heiman, M., Schaefer, A., Gong, S., Peterson, J. D., Day, M., Ramsey, K. E., Suárez-Fariñas, M., Schwarz, C., Stephan, D. A., Surmeier, D. J., Greengard, P., and Heintz, N. (2008) A translational profiling approach for the molecular characterization of CNS cell types. *Cell* **135,** 738–748

30. Nigg, E. A., Hilz, H., Eppenberger, H. M., and Dutly, F. (1985) Rapid and reversible translocation of the catalytic subunit of cAMP-dependent protein kinase type II from the Golgi complex to the nucleus. *EMBO J.* **4,** 2801–2806

31. Meinkoth, J. L., Ji, Y., Taylor, S. S., and Feramisco, J. R. (1990) Dynamics of the distribution of cyclic AMP-dependent protein kinase in living cells. *Proc. Natl. Acad. Sci. U.S.A.* **87,** 9595–9599

32. Li, L., Gervasi, N., and Girault, J. A. (2015) Dendritic geometry shapes neuronal cAMP signalling to the nucleus. *Nat. Commun.* **6,** 6319

33. Valjent, E., Corbillé, A. G., Bertran-Gonzalez, J., Hervé, D., and Girault, J. A. (2006) Inhibition of ERK pathway or protein synthesis during reexposure to drugs of abuse erases previously learned place preference. *Proc. Natl. Acad. Sci. U.S.A.* **103,** 2932–2937

34. Yagishita, S., Hayashi-Takagi, A., Ellis-Davies, G. C., Urakubo, H., Ishii, S., and Kasai, H. (2014) A critical time window for dopamine actions on the structural plasticity of dendritic spines. *Science* **345,** 1616–1620

35. Fino, E., and Venance, L. (2011) Spike-timing dependent plasticity in striatal interneurons. *Neuropharmacology* **60,** 780–788

36. Svenningsson, P., Tzavara, E. T., Carruthers, R., Rachleff, I., Wattler, S., Nehls, M., McKinzie, D. L., Fienberg, A. A., Nomikos, G. G., and Greengard, P. (2003) Diverse psychotomimetics act through a common signaling pathway. *Science* **302,** 1412–1415

37. Kuroiwa, M., Bateup, H. S., Shuto, T., Higashi, H., Tanaka, M., and Nishi, A. (2008) Regulation of DARPP-32 phosphorylation by three distinct dopamine D1-like receptor signaling pathways in the neostriatum. *J. Neurochem.* **107,** 1014–1026

38. Hamada, M., Hendrick, J. P., Ryan, G. R., Kuroiwa, M., Higashi, H., Tanaka, M., Nairn, A. C., Greengard, P., and Nishi, A. (2005) Nicotine regulates DARPP-32 (dopamine- and cAMP-regulated phosphoprotein of 32 kDa) phosphorylation at multiple sites in neostriatal neurons. *J. Pharmacol. Exp. Ther.* **315,** 872–878

39. Brami-Cherrier, K., Valjent, E., Garcia, M., Pagès, C., Hipskind, R. A., and Caboche, J. (2002) Dopamine induces a PI3-kinase-independent activation of Akt in striatal neurons: a new route to cAMP response element-binding protein phosphorylation. *J. Neurosci.* **22,** 8911–8921

40. Kuenzel, E. A., and Krebs, E. G. (1985) A synthetic peptide substrate specific for casein kinase II. *Proc. Natl. Acad. Sci. U.S.A.* **82,** 737–741

41. Kuenzel, E. A., Mulligan, J. A., Sommercorn, J., and Krebs, E. G. (1987) Substrate specificity determinants for casein kinase II as deduced from studies with synthetic peptides. *J. Biol. Chem.* **262,** 9136–9140

42. Sommercorn, J., and Krebs, E. G. (1987) Induction of casein kinase II during differentiation of 3T3-L1 cells. *J. Biol. Chem.* **262,** 3839–3843